

BiBlade Sampling Tool Validation for Comet Surface Environments

Paul Backes¹, Scott Moreland¹, Fredrik Rehnmark², Mircea Badescu¹, Kris Zacny², Robert Wei²,
Grayson Adams², Risaku Toda¹, Peter Vieira¹, Elizabeth Carey¹, Robert Krylo¹,
Miguel San Martin¹, Erik Bailey¹, Carl Seubert¹, Dylan Conway¹, Seth Aaron¹, Harish Manohara¹,
Gregory Peters¹, Marco Mongelli¹, Dario Riccobono¹

¹Jet Propulsion Laboratory
California Institute of Technology
4800 Oak Grove Dr.
Pasadena, CA 91109
Paul.G.Backes@jpl.nasa.gov

²Honeybee Robotics
398 W. Washington Blvd. #200
Pasadena CA 91103
zacny@honeybee.com

Abstract—The BiBlade sampling chain was developed for use in a potential Comet Surface Sample Return mission. Following prior versions of the sampling tool, a new tool was developed and validated to TRL 6. Sample acquisition testing was performed across a range of comet simulants and operational conditions. Tool operation was validated in a thermal-vacuum chamber. The end-to-end sampling chain was validated including sampling, sample measurement, and sample transfer. The sampling system is now ready for flight implementation.

TABLE OF CONTENTS

1. INTRODUCTION.....	1
2. BiBLADE SAMPLING CHAIN CAPABILITIES.....	2
3. SAMPLING CHAIN OVERVIEW	2
4. BiBLADE SAMPLING TOOL DESIGN	3
5. MECHANICAL POROUS AMBIENT COMET SIMULANT	9
6. SAMPLE ACQUISITION VALIDATION.....	10
7. SAMPLE TRANSFER VALIDATION.....	12
8. OPERATIONAL SAFETY VALIDATION.....	13
9. ENVIRONMENTAL VALIDATION	15
10. INTEGRATED TOUCH-AND-GO VALIDATION ...	16
11. END-TO-END SAMPLE CHAIN VALIDATION	17

12. FUTURE PLANS.....	17
13. CONCLUSIONS	18

1. INTRODUCTION

Return of a sample from the surface of a comet was identified as one of NASA’s highest science priorities in the NASA Decadal Survey [1,2]. The BiBlade sample chain was developed to acquire, measure, and store a sample from the surface of a comet in a potential Comet Surface Sample Return (CSSR) mission using a Touch-and-Go (TAG) mission architecture. A previous version of the BiBlade sample chain was built and tested [3]. This paper describes a next generation BiBlade sampling chain and validation testing. This new generation tool (Figure 1) improves upon the prior version in various ways including by doubling the sampling energy and by using flight-relevant design rules.

There are various possible mission architectures for a CSSR mission, including lander, harpoon, dart, and TAG [3,4]. The BiBlade sampling chain was developed for use in a TAG mission architecture where a spacecraft would maneuver to several meters from the surface of a small body and deploy a sampling tool at the end of a robotic arm. The spacecraft would continue descent to the surface until sample tool

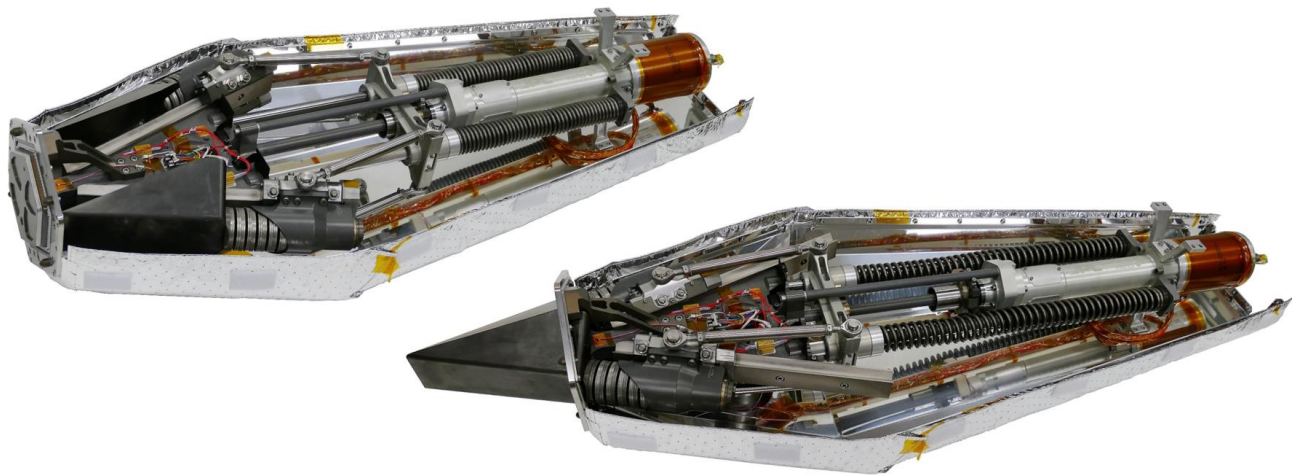


Figure 1. BiBlade sampling tool with blades open (left) and closed (right).

contact and then a sample would be quickly acquired and the spacecraft would thrust away from the surface of the small body. The BiBlade concept and several other TAG sampling tools were described and compared in an earlier publication [4]. The BiBlade was selected as the best sampling tool concept due to the unique capabilities it provides with low mission risk. The CSSR mission concept and expected science requirements were described in the Decadal Survey and associated mission study [1,2].

This paper summarizes the capabilities of the BiBlade sample chain and describes the design and validation process used to bring the sample chain to TRL 6. Section 2 lists the capabilities of the sample chain with references to the sections in the paper where the capabilities and validation of the TRL are described. Section 3 provides an overview of the sampling chain, Sections 4 and 5 describe the design of the sample chain and simulants, Sections 6-11 provide results of validation tests, and Section 12 describes future plans for the sampling chain development. Section 13 summarizes the capabilities of the sampling chain.

2. BiBLADE SAMPLING CHAIN CAPABILITIES

The capabilities of the BiBlade sampling chain are listed below, along with the sections in the paper where capabilities and TRL validation are described.

Capability	Section
Acquires comet material with strength properties from loose regolith to 5MPa cone penetration resistance (CPR).	4.2, 6
Acquires individual samples up to 500 cc volume.	4.1, 6
Acquires subsurface sample.	6
Acquires multiple samples.	3, 4.1, 4.4
Enables multiple sampling attempts per sample.	4.1
Survives sampling attempts from any strength comet material.	4.5, 8.1, 8.2
Preserves sample through benign sampling technique and maintained temperature.	4.1, 4.2, 4.7, 9
Functionality provided with only one actuator and two Frangibolts.	4.1
Prevents anchoring to comet.	4.5
Validated in comet-relevant simulant.	5, 6
Tool ready for flight implementation.	4.3, 9
Robust to spacecraft approach conditions.	6
Robust to varied surface topographies.	8.2
Safe reaction forces to spacecraft.	8.2, 10

Sampling validated with realistic spacecraft dynamics.	6
Robust operation in comet environment conditions.	9
Satisfies contamination control.	4.6
Robust sample transfer.	4.4, 11

3. SAMPLING CHAIN OVERVIEW

The end-to-end sampling chain includes sampling, sample measurement, and sample containerization.

The sampling process begins with the spacecraft several meters from the surface of a comet and the robotic arm with the BiBlade tool at its end deployed to a fixed configuration. The spacecraft then continues its descent until the sampler contacts the surface, as estimated by the GN&C subsystem, at which point the sampling tool fires, with springs quickly driving two blades into the surface of the comet thereby acquiring and encapsulating the sample, as shown in Figure 2. The spacecraft would immediately thrust away from the surface with the sample in the tool.

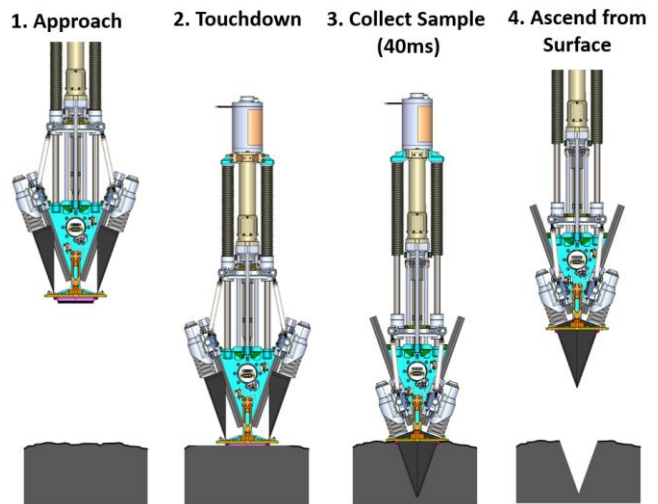


Figure 2. Touch-and-Go sampling sequence.

The sample would be measured using either a dedicated sample measurement station or by using a combination of available information including the changed surface, blade trajectory during sampling, and spacecraft motion.

A sample can be transferred to a vault in the Sample Return Capsule (SRC) or ejected. The SRC is a passive spacecraft element that is released upon return to Earth and brings the sample through the atmosphere and to the Earth's surface. For containerization the arm transfers the BiBlade to the SRC and inserts the blades into a sample vault. The blades are fully retracted and a lid is released from the BiBlade and remains attached to the sample vault to contain the sample in the vault. A second lid on the BiBlade allows for containerization of a second sample. For sample rejection, the arm extends the

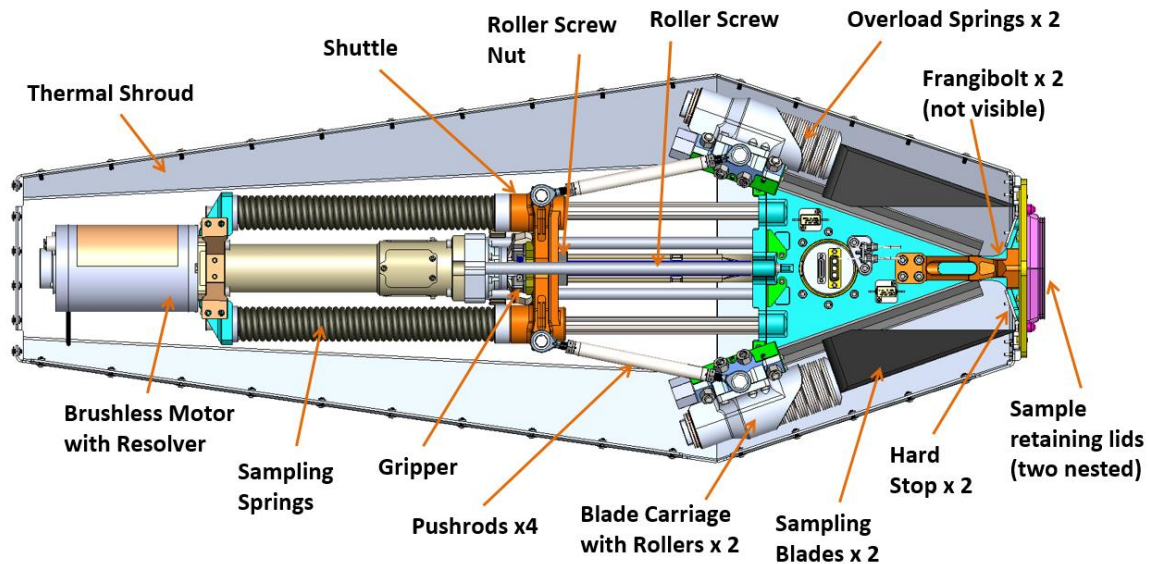


Figure 3. BiBlade primary components

BiBlade away from the spacecraft, the blades are fully retracted, and the spacecraft thrusts away thereby releasing the sample.

4. BiBLADE SAMPLING TOOL DESIGN

4.1 Functional Description

The BiBlade sampling tool has two blades that would be driven quickly into the comet surface by compression springs. The primary components of the tool are described by the process for acquiring a sample with the tool. The primary components of the sampling tool are shown in Figure 3.

To prepare the BiBlade for sampling, the actuator (brushless motor with resolver) rotates the roller screw to drive the gripper (roller screw nut is part of the gripper) into contact with the shuttle. The fingers of the gripper passively lock onto the shuttle at the shuttle latching plate, as shown in Figure 4. The actuator then pulls the gripper back which pulls the shuttle back while compressing the sampling springs. The shuttle pulls the carriages and blades up the carriage rails using the pushrods. The gripper stops just before the firing position. The gripper is then pulled back a few mm further which causes the back of the fingers to contact the rigid release plate and release the shuttle, which is then pushed down the shuttle rails by the sampling springs. The shuttle motion causes the blades to move down the carriage rails and penetrate the comet surface. The blade motion is stopped by hard stops and overload springs absorb the residual energy that was not used by the blades to acquire the sample.

Primary sampling tool properties are shown in Table 1. The 25 kg tool mass does not include structure to attach it to the robotic arm or the wrist spring.

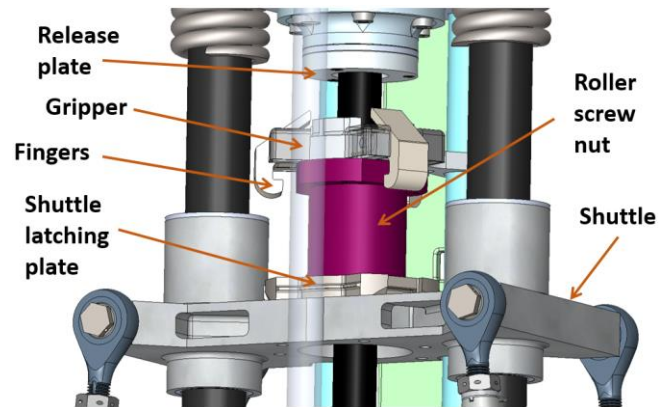


Figure 4. Grasp-release components

Table 1. BiBlade tool properties

Mass	25 kg
Length	1.13 m
Width	0.4 m
Sampling Energy (J)	300 J

4.2 Design for Sampling

From a fundamental mechanics stand-point, the BiBlade sampler is a high-speed blade penetrator interacting with brittle, porous material. As such, there is a specific set of processes that govern material failure, resistance to penetration and dynamic response. These processes are unique to the family of materials and the regime of penetration speed. Required is the study of applicable penetration mechanics theory, and experimentation and

modeling for the unique conditions if an efficient design is to be realized. A significant investigation was undertaken at JPL to develop understanding of blade penetration mechanics. Results of the work guided BiBlade penetrator properties such as accelerated mass, velocity, blade geometry and coatings. The penetration theory, experimentation and modeling work can be found in [5].

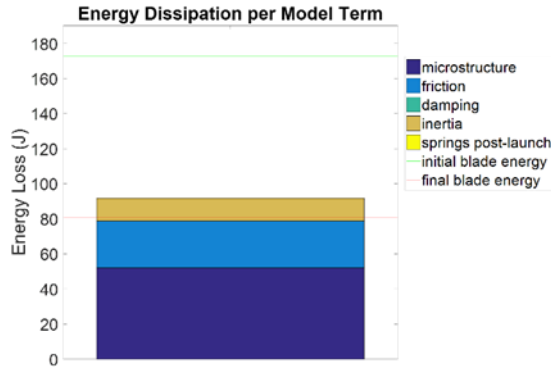


Figure 5. High-speed blade penetration of 1mm thick blade with 10m/s initial velocity.

Penetration resistance (total force required to plunge blade into material) in the speed regime of the BiBlade (0-15m/s) is a function of material microstructure strength, inertial resistance (density) and friction against the penetrator wall (see Figure 5). Blade thickness affects resistance, due to both microstructural strength and inertial resistance. An additional 5% energy dissipation was measured for every 0.1mm of additional blade thickness beyond 1mm. For these reasons, the blade thickness was minimized and a 1mm wall was implemented.

As shown in Figure 5, energy dissipation due to the inertial resistance of the material is significant. Maximum penetration velocity was reduced to 10m/s by adding dead-weights to the accelerated bodies.

Friction on the blade wall is a significant source of resistance and was studied in depth, including strategies of wide-tip leading edge and low-friction coatings. A low friction coating was implemented as it not only decreases penetration resistance but also decreases retraction/pull-out resistance. A 50% reduction in frictional resistance was realized. Blade tip geometry does not affect penetration resistance. Therefore, it was optimized to engage extremely hard surfaces such as smooth concrete to promote positive engagement (increases system safety, see Sections 4.5, 8.1, and 8.2). See [5] for in depth analysis of BiBlade penetrator parameters.

4.3 Mechanism Design and Materials

The BiBlade tool was designed in accordance with NASA and JPL spaceflight hardware standards for motor-driven mechanical assemblies. In a few cases, non-compliant materials and components were accepted in order to accelerate the fabrication schedule and enable early testing. In each case, however, a clear plan to achieve compliance

exists and a drop-in flight-like replacement has already been identified (Table 2). The result is a high-fidelity engineering unit that can readily be upgraded with no change to the existing design when increased pedigree is required. The existing BiBlade is designed to withstand a comet sampler mission environmental qualification test program as is, without these upgrades.

Table 2. BiBlade non-compliances with mitigation plans for flight.

Item	Non-Compliance (TRL6)	Mitigation Plan (Flight)
Industrial BLDC Motor	Replace bearings and lubricant, add resolver for commutation	Procure flight motor with compatible materials
Bearings/Rails	Conventional AISI 52100 bearing steel	Material upgrade to corrosion resistant 440C bearing steel
Blade trajectory	String potentiometer	Commercial flight LVDT

A partial list of NASA, JPL and aerospace industry standards used in the design of the BiBlade is included in Table 3. Components such as fasteners, bearings and springs were selected in adherence to aerospace industry specifications (e.g., NAS, NA, MS) and procured with material certifications from qualified suppliers. A partial list of flight-like materials used in the TRL 6 tool is presented in Table 4.

Since the BiBlade components would be exposed to environments ranging from ambient Earth atmosphere to temperatures as low as -40°C in the vacuum of space, corrosion resistant metals with a low ductile-to-brittle transition temperature were selected. Fasteners with locking features were used to avoid loosening and the resulting loss of preload due to shock experienced when the blades are launched. These features also keep the fasteners from loosening as a result of thermal cycling.

Table 3. A partial list of NASA, JPL and aerospace industry standards used in design of BiBlade.

Category	Partial List of Specifications	Applicability (Selected Requirements)
Mechanism Design & Analysis	NASA-STD-5017, NASA-STD-5001B, NASA-TM-106943	Actuator torque margin, structural factors of safety, general design guidelines (fastener retention, redundant springs, etc.), bolted joint analysis
Materials	MIL-HDBK-5J, AMS, MSFC-STD-3029	Material properties (strength, modulus, ductility, thermal expansion, creep, etc.), cryogenic/vacuum compatibility, specifications (materials, coatings, finishes and plating), resistance to stress corrosion cracking

Standard Parts & Fasteners	NAS/NA, MS, SAE AS, ANSI, DIN	Fasteners, nuts, inserts, rod ends, splines, bushings
Electrical	M83513, M22759, M55021	Connectors and wiring
Other		Lubricant, adhesives, paint

Nonmetallic structural materials such as wipers and the cable tray were selected for strength and ductility at low temperature and low outgassing in vacuum to minimize possible contamination of the sample. For the same reason, a minimum amount of low-temperature lubricant (Braycote 601EF) was applied by grease-plating exposed bearing surfaces of the roller screw and any accelerated mechanisms (carriage rollers, slider linear bearings). Sealed bearing surfaces were lubricated more liberally.

Differential thermal growth at critical interfaces was controlled by selecting materials with similar coefficients of thermal expansion (CTE) and by minimizing temperature differences across the body of the tool. Faying aluminum surfaces were chemical conversion coated to ensure good thermal conduction across bolted structural joints. Exposed aluminum surfaces were anodized, partly to provide protection from oxidation but also to promote desired optical properties for efficient radiative heat transfer from the thermal shroud.

Table 4. A partial list of flight-like materials in TRL 6 BiBlade.

Item	Materials
Structural members	Aluminum 6061-T6, Ti 6Al-4V
Springs	Ti Beta-C (3-8-6-4-4)
Roller Screw	CX13VD(W) Stainless Steel
Trigger Hooks	MP35N
Release Ring	C95500 bronze
Rod Ends	316, 13-8 PH
Fasteners	A-286 CRES
Lubricant	Braycote 601EF
Wipers, Wire Insulation	PTFE
Heaters	Kapton
MLI Blankets	Mylar

4.4 Sample Transfer

Located at the front end of the BiBlade sampler are the sample retaining lids for the SRC vault (Figure 3). Two lids are nested in series and are fixed to a base plate via Frangibolt non-explosive restraints (Figure 6). The Frangibolts are actuated and lid released when the sample is in the SRC vaults. Surrounding the lid baseplate a ring faceplate allows for thermal shroud mounting, blade guidance and arm shear shunts and guides during sample measurement and sample release. Between the lids baseplate and the ring faceplate is a narrow opening through which the blades travel for sampling and retrieval. This opening is covered by Teflon brushes to limit the comet material the blades bring inside the tool.

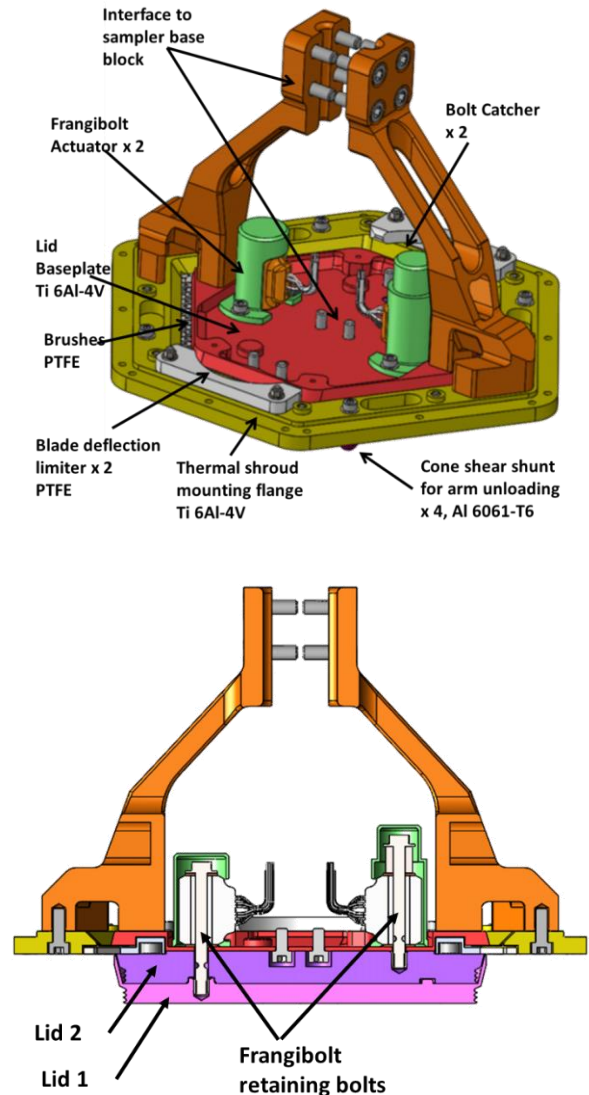


Figure 6. Lid release assembly components (top) and cross-section (bottom).

For sample transfer to the SRC, the arm aligns the tool with the SRC sample vault. The tool inserts the closed blades into the vault pressing and aligning the ring faceplate against the vault front face. Blade tapered faces guide a compliant arm in the transverse direction to align with the vault even with large positioning errors of the arm. After tool mating with the sample vault, the blades are retracted allowing the vault retention spring clips to capture the outermost lid. The cone shear shunts prevent the arm from loading the lids sideways after retracting the blades in the case of initial misalignment. With the blades retracted and the lid captured, the corresponding Frangibolt is activated, the bolt is broken and the lid is released. A vault dust seal of Nomex felt material would prevent fine particles from escaping from the vault. The arm then moves the tool away from the vault.

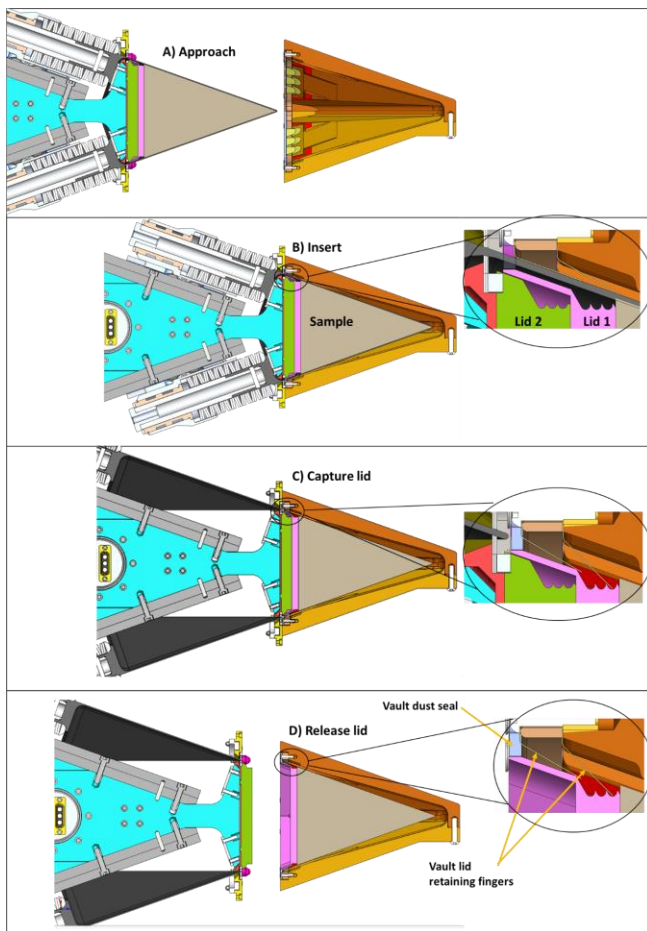


Figure 7. Sample release procedure: A) The tool with sample inside the closed blades approaches the sample vault; B) The tool inserts the closed blades with the sample into the vault and aligns the ring face plate against the vault front; C) The blades are retracted to allow the passive vault retaining fingers to capture the lid; D) The corresponding Frangibolt is activated breaking the bolt to release the vault captured lid and the tool moves away from the vault.

Two lids allow two samples to be deposited in two different vaults. The tool could have been designed with more lids for a mission that requires return of more samples. In the series of pictures shown in Figure 7 both lids are attached to the tool and lid 1 is to be released into the sample vault. Figure 8 shows the details of the Frangibolt breaking and lid release.

4.5 System Self-safety

The BiBlade sampler has design features to achieve robustness against the following: (1) Hard surface impact damage, (2) Touch-and-Go motion induced forces on the sampler, (3) inducing undesirable loads to spacecraft, (4) trapping of blades in comet surface, and (5) dust/debris.

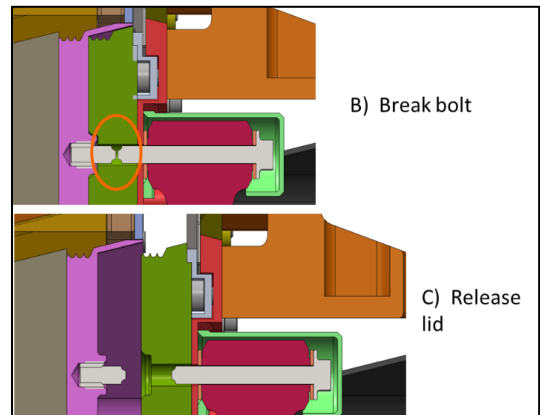


Figure 8. Lid restraint release details.

Impact Protection Mechanism

The BiBlade is designed to survive firing into vacuum and into perfectly rigid objects, which are bounding worst cases for structural survival since all sampling energy is absorbed internal to the tool.

Figure 9 displays the overload/isolation springs that exist at the base of the blades. All moving mass other than the blades become sprung and do not encounter significant loads. The overload springs are preloaded to 2.5kN. The two bodies (1. blades, 2. everything else) are intentionally quite different in mass (0.35kg and 5.35kg respectively). Additionally, the overload/isolation spring rate and the blade stiffness are an order of magnitude different. The springs act as isolators separating the blade body impact and the remaining 5.35kg body impact (Figure 9). Two dynamic events, at 2 kHz and 0.1 kHz occur, therefore the total load is reduced. As the blade body is relatively stiff, a high impact event occurs and dominates compared to the 0.1 kHz event. Essentially, the high load impact is solely created by the mass and velocity of the blade (stand-alone body from rest of system). To minimize the peak force, the kinetic energy in the blade body is minimized by limiting the blade velocity and minimizing mass. To do so, a limit of 10m/s of the accelerated bodies is made by adding dead-weight to the roller carriages (not blade body). This results in maximum kinetic energy in the blade (and the 2 kHz impact) only being 17.4J (per blade). Compare this value with 265J in the sprung body.

When the BiBlade is fired into empty space or there is residual energy after sampling, the same overload spring mechanism strikes a hard stop and arrests motion safely. The load path does not go through the blade body in this case but only through the high-strength base portion of the component. The sampling energy is then safely absorbed internally to the tool.

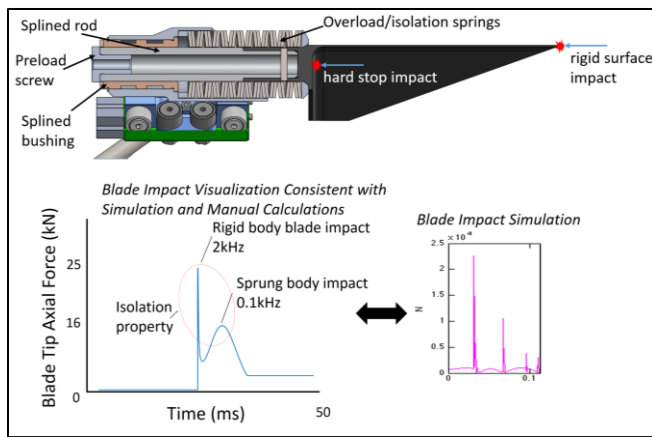


Figure 9. Design of the blade impact load protection system. A preloaded stack of disk springs (Titanium BetaC) compresses if larger than nominal sampling forces are encountered. It acts to reduce impact forces and isolate blade body impact from sprung body impact loads.

Static testing of blades (Figure 10) was conducted to verify the buckling mode and critical load for validation of an FEA model to be used for static/dynamic analysis. See Section 8.1 for validation of this topic.

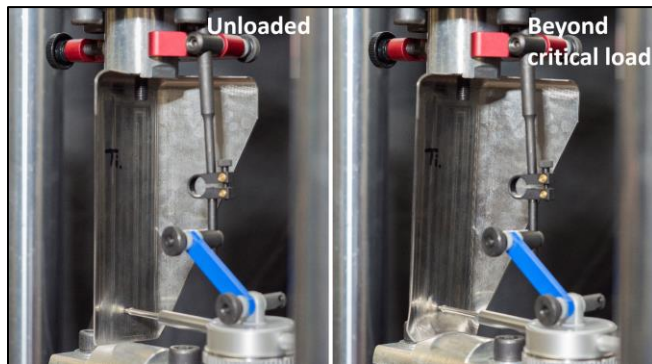


Figure 10. Static testing of spare titanium blade from prior prototype on Instron machine. A point load at the center of the blade tip induced by an aluminum half-round generated this worst-case load condition (buckling).

Wrist Spring

A compliant wrist joint is located at the end of the BiBlade as an interface to the robotic arm. This component is made up of a single spring with its long axis oriented collinear to the sampler's long axis. This wrist joint consists solely of a spring with structural flanges on both ends. There are no explicit rotary mechanisms such as bearings or bushings. Note that the wrist spring does not deflect in the axial direction (compression direction) but does have angular articulation via bending. The effective spring rate is 2Nm/degree.

The wrist spring has two functions: (1) limit blade moment induced by spacecraft transverse motion, and (2) reduce spacecraft angular rates induced by the BiBlade when striking an oblique hard surface.

In Touch-and-Go operations spacecraft lateral motion could exist when the blades are engaging the comet surface. The wrist spring compliance allows lateral motion of the spacecraft without exceeding structural capability of the blades.

The wrist spring mitigates the effects of moments imparted to a spacecraft if the blades strike a smooth, rigid surface at an oblique angle. Also, the blade edge would dig into the comet surface to dissipate sampling energy. Multibody simulations of the full sampler-spacecraft system were used to specify spring rate properties and mature the wrist spring concept that was eventually validated experimentally (Section 8.2). The wrist spring decouples the sampler body from the spacecraft body leading to a small fraction of momentum being transferred to the spacecraft body, while the blade edge and overload springs positively engage the surface and dissipate large amounts of energy into non-rotating form. See Section 8.2 for validation.

Robustness to Blade Trapping

Blade geometry and blade pull-back capability prevent anchoring to the comet. The closed blades form a fully tapered shape so the blades release from the comet with any vertical motion. If the blades do not fully close and remove the sample, the actuator has enough torque to execute an abort procedure to pull back the blades and break the comet material, thus freeing the blades. In an abort procedure, the roller screw nut with the gripper would be driven to grasp the shuttle to pull the blades free from the comet.

In the analysis, the blades are assumed to be partially driven into the comet material and the material exerts both on the inside and the outside of the blades a pressure equal to the compressive strength of the comet material (the maximum pressure the material can support). Twenty percent of the comet material is assumed to be of a sticky nature and needs to be sheared to let go of the blades. A friction coefficient of 0.18 between the DLC (diamond like coating) Ti coated blades and simulant material was determined from testing. When the blades are pulled for extraction, shear forces for 20% of the surface and friction for the rest of the surface prevent the blades from moving. In addition to the force required to extract the blades, the actuator needs to overcome the drive springs compression as well.

In a parallel development a single blade penetration testbed determined the blade penetration depth as a function of the material strength given a predetermined kinetic energy. Details of the penetration mechanics study can be found in [5]. The penetration depth was used to determine the maximum retraction force (blades extraction plus the drive springs compression) for every material with an unconfined compressive strength in the range of 0 to 50MPa. The plot of

these max values is shown in Figure 11. A peak value of 8kN retraction force was calculated to be required to extract the blades from the comet material in the assumed conditions and the actuator was designed to provide this force with design margins.

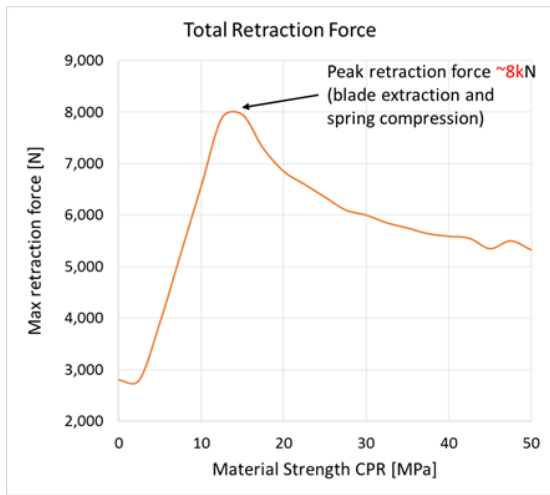


Figure 11. Total retraction force required.

Dust/debris

The BiBlade was designed to operate robustly in a high dust and debris environment. The thermal shroud acts as a first line of defense and covers the whole sampler other than a 3mm hexagon slot at the front end of the sampler where blades pass through. This slot is protected by three layers of PTFE seals (Figure 12) that wipe the blades, and prevent material from entering when interacting with the comet surface. In addition to the PTFE seals, rigid break-off features exist if particles are strongly adhered to the blades (i.e. knock off large particles). As a back up to the wiper/breakers, all internal exposed mechanisms are tolerant of operating in an environment with hard particles up to 1.5mm (gripper/release mechanism is an example). Meanwhile, the large diameter carriage rollers are capable of crushing all simulants tested if particles this size are present on the rails. All other components have seals and/or wipers.

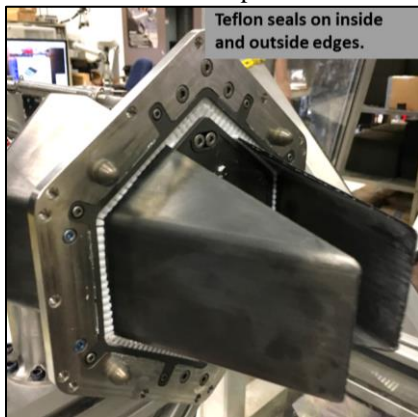


Figure 12. Close-up of dust/debris seals that wipe blades and close off only opening not covered by thermal shroud.

4.6 Contamination Control

The BiBlade was designed to be compliant with contamination control requirements that would be needed for a CSSR mission. The following strategy was implemented for the BiBlade prototype: select compliant materials where possible, contain non-compliant materials, and bound maximum ppm of non-compliant material. There are two primary sources of contamination, Braycote 601 EF lubricant and the sampling blade coating. All remaining materials of the BiBlade were considered compliant materials as reviewed by JPL experts.

Braycote lubricant was minimized by using a 90%-10% grease plating process. This deposits a very thin coating of lubricant via evaporation process, thus minimizing total contaminant volume (weighing parts before/after process measured total mass). Grease plating also achieves high adhesion thus reducing migration.

Conventional bearings were grease plated (thus using minimal contaminant) and sealed. Braycote located in accelerated/decelerated components was also in the grease plate form but contained via enclosures and ballistic shields. Together, minimization via grease plating, implementation of enclosures and ballistic shields provides an approach consistent with JPL contamination control methods. See Figure 13 for diagram of accelerated body ballistic shields.

The blade coating was considered a possible contaminant but then deemed compliant, as the total mass expected to get into the sample is low. The diamond-like carbon coating (hydrogenated amorphous carbon a-C:H) is acceptable as manufacturers adhesion tests and BiBlade testing showed it doesn't wear or flake off. Bounds for coating contaminant level (assuming 1% of coating will fall into a 500cc sample) would be 2.4ppm by volume. This was confirmed an acceptable value.

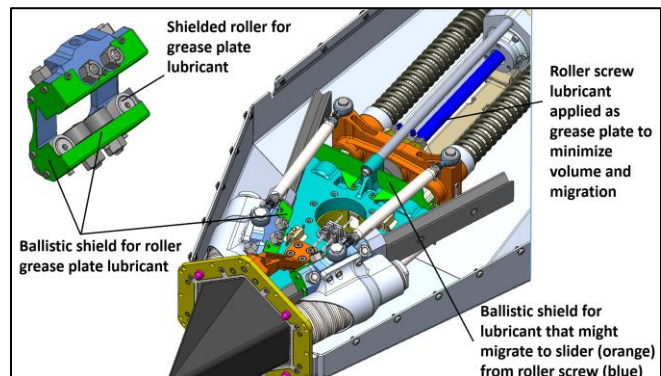


Figure 13. Implementation of shielding as part of the contamination control strategy for lubricants. Multiple layers of shielding contribute to minimize contamination.

Cross contamination between samples is minimized by having the blades cleaned off each time they are retracted into the sampler body. The wipers are shown in Figure 12.

4.7 Thermal Control

The BiBlade was designed to operate in the thermal environment expected to be found at a comet located 4-5AU. For design requirements, this is a 70K black body sink with no solar flux (all exposed surface low absorptivity). The thermal control system was designed to keep all sampler components within their allowable flight temperatures and maintain surfaces contacting the sample below -25°C so as to not cause alteration (science requirement). The design was specified for steady state and transient heating operations (motor usage). The primary thermal control components were.

- Rigid aluminum thermal shroud with mirror-like internal finish
- 15-layer MLI blanket shroud cover
- Two heating circuits with Honeywell 706S-27A-14 preset thermostats, film motor heater and base block power resistors (as heaters)
- High thermal resistance structural interface to wrist-joint/robotic arm

See Figure 14 annotation for more detail. All thermal control components were flight components drawn from JPL flight inventory.

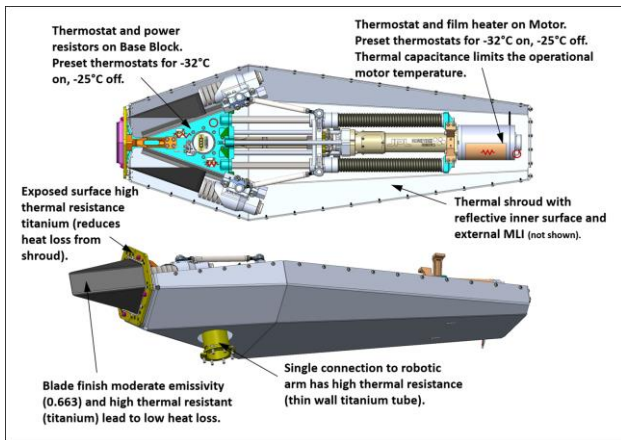


Figure 14. Diagram of thermal control system elements implemented and validated in BiBlade prototype.

Finite Element Analysis (FEA) thermal modeling of the BiBlade was conducted prior to final construction of the sampler. Critical bodies and interfaces were modeled including (Figure 15), heated/temperature controlled motor, heated/temperature controlled base block (primary structure), blade interface, blade, rigid aluminum shroud, shroud MLI (blanket insulation), and the robotic arm interface. The model was configured to analyze heated element power requirements and allowable flight temperatures for critical bodies (including blade maximum temperature)

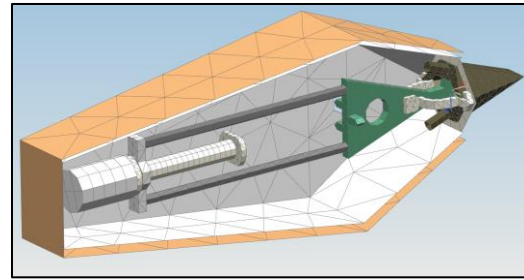


Figure 15. FEA thermal model of BiBlade sampler.

The model shows that the blades would be maintained below -25°C with large margin (to prevent sample alteration), while allowable flight temperatures of components are met. See Figure 16 for results. The thermal control system was validated during a full sampling system thermal-vacuum test with background temperature of -160°C as described in Section 9 for thermal-vacuum test validation.

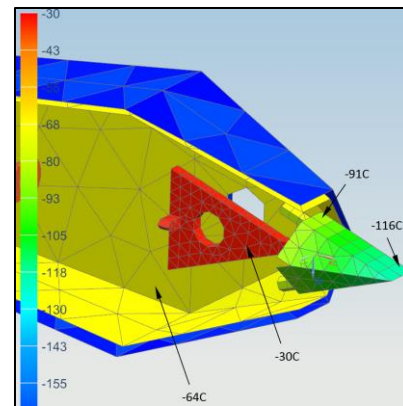


Figure 16. Thermal model results of steady state condition.

4.8 Minimization of Ejecta

Minimization of ejecta caused by sampling is important to limit the amount of ejecta that could transfer to spacecraft surfaces. Two primary design features minimize ejecta generated during the sampling process. First, use of thin blades for penetration minimizes the energy imparted during the sampling process. Second, during the approximately 40ms of the sampling process the forward momentum of the blades causes the tool body to slightly recoil away from the comet.

5. MECHANICAL POROUS AMBIENT COMET SIMULANT

A suite of simulants was developed to represent a range of potential comet properties. A mix design called Mechanical Porous Ambient Comet Simulant (MPACS), as shown in Figure 17, was developed using Portland cement and pumicite combined and added to water and a foaming agent [7]. Strength properties were varied by changing the amount of foaming agent added to the mixture. The MPACS material

was fabricated into 8-inch cubic boxes for the BiBlade test program. Density, cone penetration resistance (CPR), uniaxial compressive strength (UCS), shear strength, and porosity were measured.



Figure 17. Mechanical Porous Ambient Comet Simulant (MPACS) simulant block.

The mechanical properties of the MPACS and Foamglas simulants used in the sampling tests are shown in Table 5.

Table 5. MPACS and Foamglas test simulant mechanical properties.

	MPACS 'F'	Foamglas T4	Foamglas HLB1600 'F'
CPR [MPa]	5.0	0.4	3.9
UCS [MPa]	1.0	0.5	12.4
Density [g/cc]	0.42	0.09	0.15
Porosity [%]	84	>95	>95

6. SAMPLE ACQUISITION VALIDATION

The validation of BiBlade sample acquisition performance was conducted utilizing a testbed designed to account for interface and operational scenarios, and a suite of simulants including in-house manufactured and material used by other agencies for prior missions [8].

Validation of BiBlade sample acquisition confirmed

- Collection of sample volumes of 250cc to 500cc with at least 75cc below 4cm of the surface
- Capture of material up to a strength of 5MPa cone penetration resistance (CPR) of relevant simulant - MPACS
- Robustness to local surface slope angle
- Compatibility with interfaces and full-system properties including stiffness and spacecraft inertias
- Robust to approach velocities up to combined 4cm/s axial and 4cm/s transverse
- Clean capture to enable Touch-and-Go ascent operation

978-1-5090-1613-6/17/\$31.00 ©2017 IEEE

of spacecraft (pull-out force <25N, full blade closure)

The Sample Acquisition System Testbed (Figure 18) was used for most of the BiBlade tests. Key features of the testbed are (1) linear actuator representing spacecraft approach velocity (any angle), (2) planar representation of wrist spring pivot interface, (3) representation of full spacecraft inertia via flywheel geared to 2200kg, and (4) simulant surface orientation adjustability.

Due to space limitations of the publication, only results of the enveloping test configuration are presented. These represent worst-case operational scenarios and act as conservative results when reporting BiBlade capabilities.

The test configuration was as follows

- Sample Acquisition System Testbed
- 5.7cm/s approach velocity at 45° (equivalent to 4cm/s axial and 4cm/s transverse)
- 2Nm/degree wrist joint spring
- 2.5-5MPa CPR MPACS, 0.5 CPR Foamglas T4, 3.9MPa CPR Foamglas HLB1600 ("F")

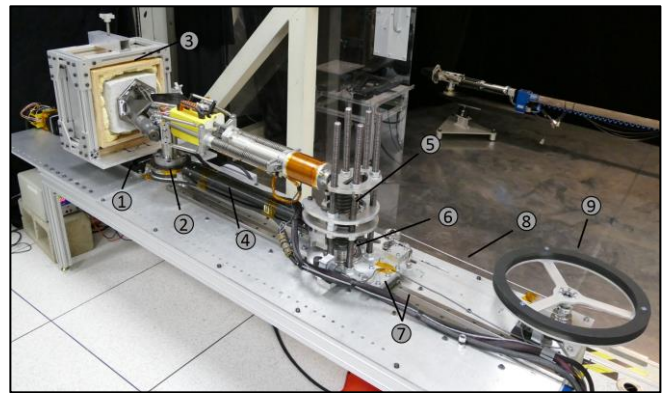


Figure 18. Sample Acquisition System Testbed utilized for validation and characterization of sampling performance. Critical parts consist of (1) "approach velocity" linear stage with adjustable pointing direction, (2) force/torque sensor, (3) simulant fixture, (4) sampler/spacecraft connecting tube, (5) tunable spring loaded pivot (represents wrist spring), (6) pivot cross-roller bearing, (7) ball bearing carriage (2x) and rail for axial motion, (8) cable for load transfer to flywheel, (9) flywheel representing 2200kg S/C inertia, *not visible are four position sensors.

Weak surface layers such as dust are possible on comets and may overlay a harder layer where recondensed water ice increases locally the materials strength [8,9] Tests investigating the capability of sampling MPACS of 5-6MPa CPR (binned as 5MPa) included an approximation of the effect of a dust layer over the stronger material. Little energy is expended on the weaker upper layer, therefore larger sample volumes or stronger sub-layers can be acquired. The dust layer was represented by a stand-off from the material surface. Figure 19 displays the test results approximating the

effect of a dust layer. Results show the capability of the BiBlade to acquire 300cc of 5 MPa material with as little as 2cm of dust and 450cc of material with 5cm of dust.

Results of the sample acquisition tests are plotted in Figure 20. The blade end of travel penetration rate (blade velocity) and sample volume acquired are metrics used to determine capability. The results of two pass-fail metrics were also recorded but not displayed since all test results were positive for the range of strength. Failures were only observed above 5.6MPa CPR, however graceful degradation occurred. These metrics were (1) blade full closure and (2) pull-out force <25N. The latter would be equivalent to a maximum thruster force a spacecraft might have to ascend from the surface.

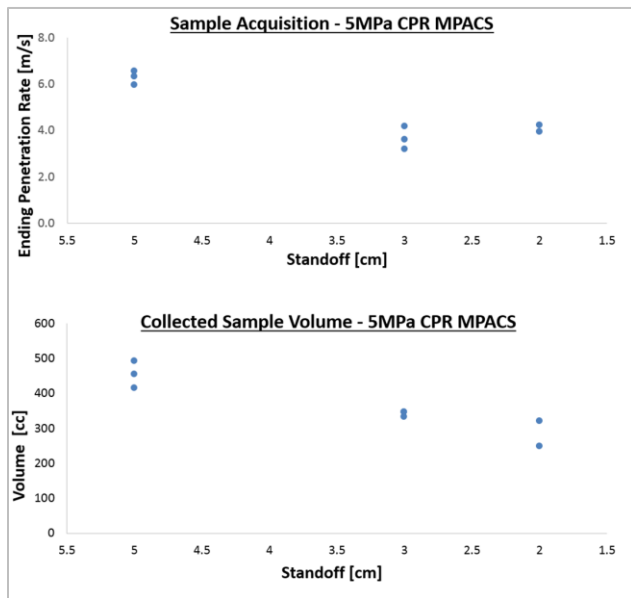


Figure 19. Sample acquisition system testbed results with dust layer simulated as standoff from surface. With as little as 2cm dust (i.e. weak material), the BiBlade can collect 250cc to 450cc of 5 MPa CPR MPACS.

About 500cc of sample was acquired for 2MPa MPACS and about 250cc of sample was acquire for 4 MPa MPACS, which would represent 7cc below 4cm depth. At this material strength, the blades still maintain an end of travel speed of 2-3m/s (initial speed 10m/s).

The Sample Acquisition System Testbed was deemed overly conservative when reporting BiBlade performance. This is due to excessive deflections of low stiffness components such as the flywheel cable. Although efforts to increase rigidity where made, high speed camera analysis shows total deflections greater than 2cm for 4-5MPa CPR simulants. The BiBlade would be expected to have higher sampling capability when mounted to a system with a more direct load path to the 2200kg mass, as is expected for a CSSR mission. A full-scale spacecraft testbed is being constructed (Figure 36) at JPL to support testing of the BiBlade sampler with the more realistic stiffness between tool and spacecraft.

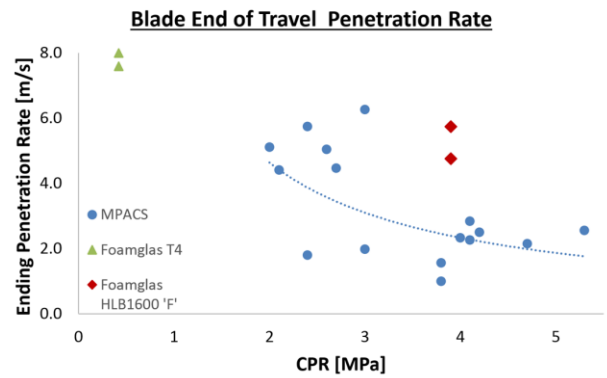


Figure 20. Sampling validation results from Sample Acquisition System Testbed. Configuration for all tests were with touchdown velocities of 4cm/s axial and 4cm/s transverse combined and tool perpendicular to simulant surface. This configuration is representative of the most difficult scenario with respect to other touchdown velocities and surface topologies.

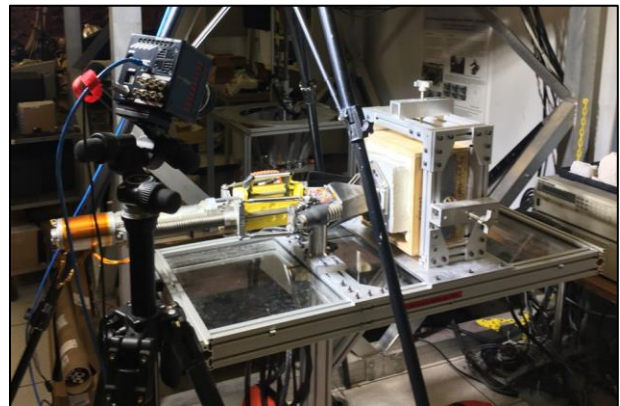


Figure 21. BiBlade sample acquisition testing with Rigid Testbed. Both the sampler base and simulant block are rigidly fixed. In this configuration, the BiBlade was shown to reliably sample 5.0+MPa CPR MPACS simulant but an upper limit of 7MPa was demonstrated.



Figure 22. Shown is an acquired sample of a 5.2MPa CPR MPACS simulant block from the Rigid Testbed. The hole created reached 15cm depth and acquired a mostly intact 520cc volume sample. The blade end of travel velocity was 5.5m/s (at full blade closure). Four tests ranging from 5.2 to 5.6 MPa CPR were repeated with similar results.

The Rigid Testbed was used to evaluate the BiBlade when both the sampler and simulant block are fixed (Figure 21). In this configuration, the BiBlade reliably sampled 520cc volumes of 5MPa CPR MPACS simulant (Figure 22).

A test was performed to acquire fly ash to validate acquisition of weak material and to assess the generation of ejecta during sampling, as shown in Figure 23. The prior version of the BiBlade was used, but the blade speed was the same as for the current BiBlade. Fly ash is an unconsolidated and fluffy material with negligible strength.



Figure 23. Sampling fly ash.

The test validated that the BiBlade fully acquires very weak material. The picture in Figure 23 is from the moment when the maximum amount of ejecta can be seen. It shows a small amount of ejecta, but it is believed that the primary cause of the ejecta was disturbance of the fly ash from the air that was pushed forward by the blade motion. A better test for ejecta generation would be done in a vacuum chamber to eliminate the effect of air movement and at micro-gravity so gravity does not affect the ejecta motion. These tests are being considered for follow-on work.

The BiBlade sample acquisition capabilities have been verified to meet the following attributes.

- Collection of sample volumes of 250cc to 500cc with at least 75cc below 4cm of the surface
- Capture of material of strength 0-5MPa cone penetration resistance (CPR) of relevant simulant - MPACS
- Compatibility with Touch-and-Go like operations with full-system properties including spacecraft inertias and velocities (4cm/s axial and 4cm/s transverse)
- Clean capture to enable ascent operation of spacecraft (pull-out force <25N, full blade closure)

The sample transfer testbed consists of a robotic arm, the BiBlade and the Sample Return Capsule (SRC) vaults (Figure 24). The SRC for a CSSR mission is anticipated to have heritage from the Stardust, Genesis, and OSIRIS-REx missions. It is the Earth entry vehicle that carries the sample through the Earth atmosphere and until retrieval. Mechanical compliance of the robotic arm and tapered blades allow the sampler blades to act as large alignment features enabling robust insertion into the SRC vault and attachment of the lid.

7. SAMPLE TRANSFER VALIDATION

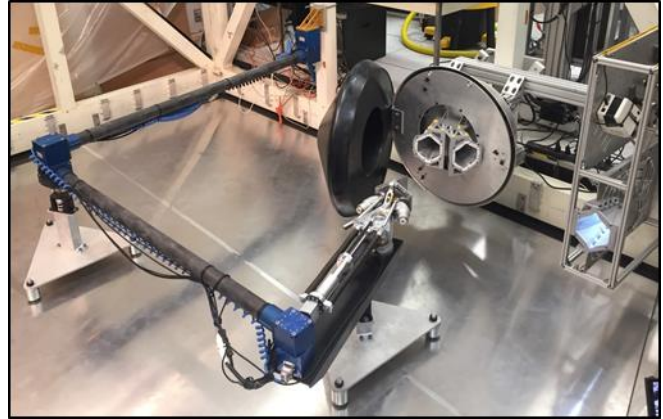


Figure 24 Validation of sample transfer using high fidelity testbed. Includes weight off-loaded 3-DoF robotic arm of representative stiffness, BiBlade with Frangibolt actuator lid restraint, and SRC geometric mock-up with two sample vaults.

There were four aspects characterized and/or validated during the testing:

- Use of Frangibolt non-explosive actuators for lid restraint (shock considerations)
- Translational/rotational initial misalignments
- Hard inclusions and protrusions between blades

Frangibolt actuation (non-explosive bolt breaker) was included in each test to verify shock induced does not affect lid capture.



Figure 25. Validation of robustness to robotic arm misalignment during insertion of BiBlade into SRC vault. Linear and angular offsets were introduced and proper lid deployment and capture was verified. A 4cm transverse offset (left figure) and 5° angular offset (right figure) are shown to have no adverse effects on sample transfer.

To validate robustness to robotic arm positional error, axial and transverse offset were introduced and angular offset were introduced (Figure 25). It was verified that 4cm transverse/axial misalignment and 5° angular misalignment with the SRC do not prevent the sample from being

successfully transferred to the SRC vaults and the lid fully engaging the locking features.

Robustness to hard inclusions stuck between the blade edges and sample material protrusions was verified (Figure 26). Rocks up to 2cm in diameter were placed between the blades. Rigid protrusions were created by sampling MPACS simulant of 9MPa cone penetration resistance and shards manually orient to protrude from the blade. Robustness to these scenarios were designed into the SRC vaults via special geometry.

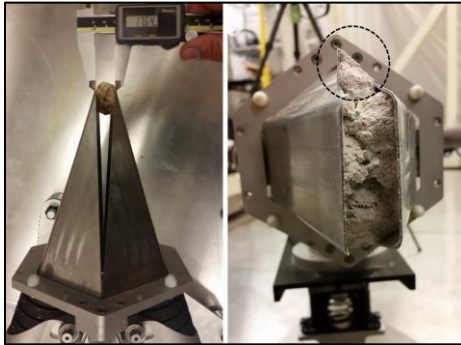


Figure 26. Validation of sample transfer/containerizing robustness to large inclusion between blade edges creating gap or deflection and protrusions. Rocks (left figure) and comet simulant protruding shards (right figure) where intentionally place between blades. Scenarios shown successfully transferred to the sample vault.

Summary of successful sample transfer validation with the following attributes:

- 3DoF planar robotic arm with relevant stiffness and open-loop position control
- Use of Frangibolt non-explosive actuators for lid restraint (shock considerations)
- Translational/rotational initial misalignments up to 4cm axial and transverse misalignment, 5° angular misalignment
- Hard inclusions between blade edges of 2cm and protrusions between blades up to 4cm
- Lid locking features

An example of a transferred sample and close up of the SRC geometric mock-up is provided in Figure 27.

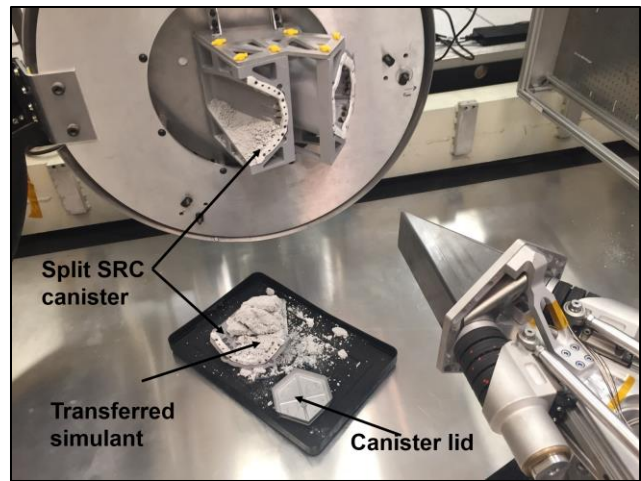


Figure 27. Example of transferred sample manually removed from SRC vault. Sample vault is disassembled into halves to allow disengagement of lid locking features.

8. OPERATIONAL SAFETY VALIDATION

The BiBlade is designed to self-protect against damage to itself and the spacecraft. The primary features to do so are (1) the blade impact overload/isolation mechanism, (2) the wrist spring and (3) blade pull-out/abort capability via high torque actuation and low resistance coating blades. This section provides validation of the blade impact protection and spacecraft load transfer reduction.

8.1 Self-safety Results

The structural integrity of the blades and function of the impact overload/isolation mechanism was verified via full system testing of the BiBlade while striking a high rigidity object. The blades and the overload/isolation mechanism are designed to prevent damage to all parts of the BiBlade when striking a rigid surface at maximum blade velocity. Maximum velocity is reached when there is 15cm stand-off between the BiBlade front plate and the surface of the struck object.

As a worst-case interaction, the tests were configured so only one blade strikes the test surface. This imparts almost the full 300J of the sampler through a single blade load path. The surface struck was a concrete cinder block. The relatively smooth cinder block selected was considered by scientists to be highly conservative with respect to surface smoothness that could potentially exist on a comet. Figure 28 shows a test at the moment of the blade impact. Post-test visual inspection showed no damage to the blade or any component of the sampler. These tests validated the feature of the sampler that it may strike a surface of any hardness and not lead to self-damage.

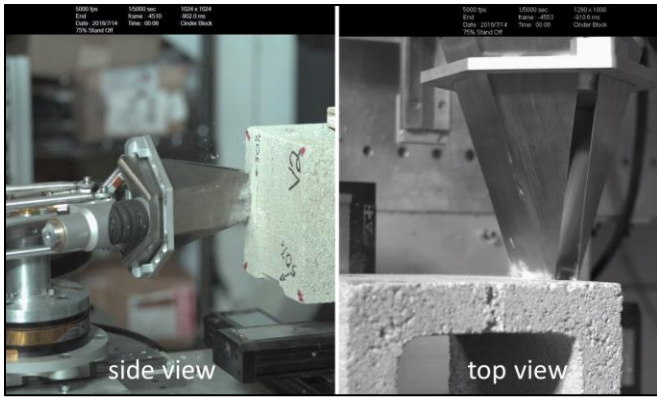


Figure 28. High speed video frames of blade survivability verification during impact. The worst case scenario was configured consisting of a high stiffness material (cinder block), maximum stand-off (highest kinetic energy in blades) and single blade interaction. Only one blade hits the block. The overload/isolation mechanism successfully prevents damage to the blades.

8.2 Oblique Strike Results

Striking of a smooth, rigid surface at an oblique angle could impart significant side loads to the blades and a moment about the spacecraft. Two aspects of the BiBlade design are intended to alleviate this potential issue. These are the wrist spring and the anchoring effect that the blade edges create when striking even a sloped surface.

A planar representation of the wrist spring was created for the Sample Acquisition Systems Testbed. This consisted of a pair of counter loaded torsion springs and a cross-roller bearing that was capable of being reconfigured with different spring rates and preload. A planar implementation was used since the wrist spring would not support testing in 1-g.

Multibody simulations of the full sampler-spacecraft system were used to select the spring rate to evaluate. A spring of 2Nm/degree was selected. A wrist spring of equivalent rate was fabricated so it could be used in the gravity off-loaded full-scale testbed (Figure 36). The sampler-spacecraft full system simulation also indicated that a 45-degree surface angle is of worst case. Figure 29 shows the testbed configured for the oblique strike scenario validation.

The BiBlade fired into the 45° cinder block four times to validate blade survivability and measure energy that would be transferred to the spacecraft via moment transfer that would contribute to angular rate, with results shown in Figure 30. Validation of the structural integrity of the blade was confirmed via visual inspection. Only minor scratching in the form of <1mm yielding occurred on the blade tip.



Figure 29. Validation testing of energy transferred to S/C during rigid surface oblique strike scenario. Shown is a rigid, smooth surface (cinder block) fixed at 45° to the BiBlade sampling axis with the face of the sampler touching. This configuration represents the worst-case scenario for blade interaction with a surface that may lead to excessive spacecraft rotational rate.

The rotational energy of the BiBlade pivoting about the torsion springs was measured to evaluate energy that may be transferred to the spacecraft leading to angular rates. The energy was measured two different ways. First by measuring the angular rate of the BiBlade with no torsion springs attached and the second method was to measure the energy stored in spring deflection (i.e. maximum angle of rotation).

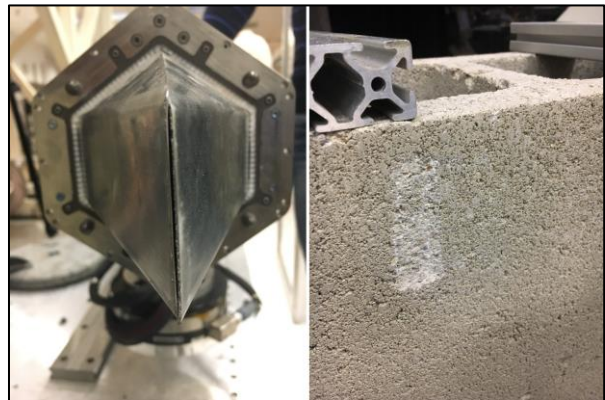


Figure 30. Inspection post-test of the oblique strike scenario shows that the blades are undamaged. The point of the blade tip promotes positive engagement of the smooth cinder block surface.

It was determined that most energy was lost during the surface impact interaction (high frequency vibration of components, cinder block chipping and overload spring compression). Table 6 lists the energies calculated for each oblique strike test. Typical values of energy transferred to the rotation system were under 6J while the last test was 19J due to significant blade sliding. This was due to the blade edge being sanded down during multiple tests, therefore not able to positively engage the cinder block surface.

Table 6. Rigid, smooth surface oblique strike test results measuring the dynamic response as rotational energy that could be transferred to spacecraft.

Test	Maximum Angular Rate of Sampler [deg./s]	Maximum Spring Deflection [deg.]	Energy via Initial Angular Rate [J]	Energy via max. Torsion Spring Compression [J]	Pushback Force X, Y [kN]
1 – no spring	52	N/A	6	N/A	2, 0.7*
2 – w/ spring	34	4.4	3	4	-
3 – w/ spring	75	4.7	12	5	2, 0.7*
4 – w/ spring, blade slid	115	14.7	28	19	2, 0.7*

* $\tan^{-1}(2/0.7) = 19\text{deg}$ (blade angle)

Results indicate that $\ll 10\%$ of the sampler’s compressed spring energy is transferred to the BiBlade-wrist spring system. For a $5500\text{kg}\cdot\text{m}^2$ spacecraft the rotational rate would be 5.8 degrees/s assuming 100% momentum transfer. However, applying simple moment/energy transfer equations yields only $1/16^{\text{th}}$ the energy of the BiBlade-wrist spring pivot system would be transferred to the spacecraft. Therefore the expected maximum angular rate of the spacecraft due to oblique strike of a smooth, rigid object is 1.4 degrees/s. This result validates the ability of the sampling system to protect the spacecraft from BiBlade induced angular rates in even highly conservative worst-case scenarios.

9. ENVIRONMENTAL VALIDATION

The BiBlade was designed to operate in thermal and pressure environments expected at comets up to 5AU from Earth as well as near earth thermal loading. Thermal-vacuum testing was conducted to validate the environmental design aspects and to quantify system performance in a flight-like environment (Figure 31). A custom cold-shroud of much smaller size than the vacuum chamber was constructed to achieve very cold temperatures by reducing the thermal mass required to cool and by minimizing radiative losses. A slot allowed for high speed video (5000fps) of the blade motion. The number of thermal cycles of the test is consistent with design practices for the type of hardware and orbital profile of a comet mission.

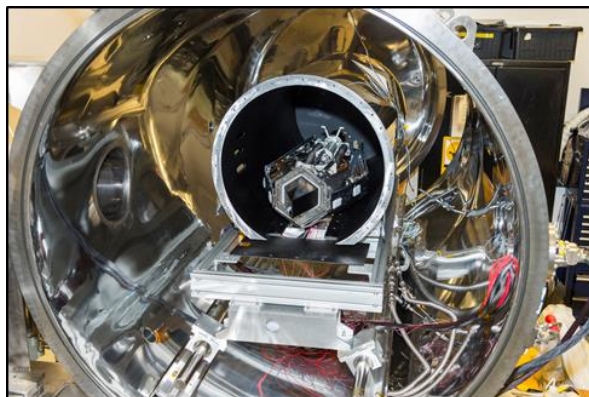


Figure 31. Environmental testing of BiBlade in thermal-vacuum chamber. Cold shroud end plate and top half of BiBlade thermal/dust shroud removed for photo.

Thermal-vacuum test configuration:

- Cycling between $+70^{\circ}\text{C}$ and -160°C (three cycles)
 - High power AC heaters on sampler to bring sampler internal temperature to $+70^{\circ}\text{C}$
 - Cold shroud avg. temperature -160°C (measured by four thermocouples)
 - Sampler thermal control system maintained internal temperatures during the cold phase between the thermostat set points, -32°C to -25°C
- Pressure 10^{-7} torr (high vacuum)
- Functional testing
 - Perform actuator homing operations at each cold cycle
 - Functional test at last cold phase consisting of self-fire sampling operations five times
- Performance verification
 - Verify thermocouples read values within allowable flight temperatures of the components
 - Verify surfaces contacting sample (blades) do not exceed -25°C
 - Verify that actuator maintains adequate torque/current margin
 - Verify kinetic energy available for sampling (blade speed) within 5% of Standard Temperature/Pressure condition

The sampling system - actuator and mechanisms - and thermal control system functioned as designed during all aspects of the thermal-vacuum tests.



Figure 32. Temperature of critical components during cold/vacuum operation testing with -160°C cold shroud. Measured temperatures (see red dots for locations) were consistent with component allowable temperature limits and requirement of sampling surfaces (blade) to maintain temperature below -25°C .

The thermal control system maintained components within their specified allowable flight temperatures; including observing the -25°C blade upper limit with a 10°C margin. Figure 32 provides temperature measurement of critical locations within the BiBlade. Once the internal temperature of the sampler reached steady state, the blades were retracted to firing position, held in this position for five minutes and then temperatures recorded. The blade retraction hold is a required operation that inadvertently raises the temperature

of the blades slightly due to retracting into the sampler debris/thermal shroud.

Design validation and quantification of degradation due to expected temperature effects was completed. The sampling system was evaluated in two parts, (1) the actuator and roller screw mechanisms related to blade retraction (compressing the firing springs) and (2) the accelerated bodies, blades and associated mechanisms that store kinetic energy during the sampling penetration process. Table 7 reports the blade end of travel speed and the actuator torque/current margins for standard temperature/pressure and at the thermal-vacuum, test cold conditions.

The blade speed metric represents kinetic energy available in the blade for sampling. The test results (Table 7) show little degradation in potential sampling ability while functioning in the $-160^{\circ}\text{C}/10^{-7}$ torr environment. An average loss of speed and kinetic energy was only 1% and 2.5% respectively. A minimum actuator torque/current margin of 181% was recorded therefore exceeding the 150% margin requirement. Although the torque/current margin of the actuator was much less than at standard temperature/pressure, this was expected when operating Braycote lubricant in the -40°C range.

Table 7. Environmental validation functional test results. Energy transfer to blade and actuator torque/current margin are metrics in cold/vacuum conditions.

	Standard Temperature/Pressure	Environmental Conditions, $-160^{\circ}\text{C}/10^{-7}$ torr
	Blade End of Travel Speed [m/s]	
	10.43	9.68 9.87
	9.80	9.47 9.73
	9.87	9.37 9.81
	9.68	9.64 9.73
	9.47	9.52 9.03
	9.37	9.78 9.35
	9.64	10.63 9.28
average	9.75	9.66
st. dev.	0.34	0.40
	Actuator Torque/Current Margin [%]	
	500	181
	429	200
		200
average	465	194
st. dev.	49.9	10.8

10. INTEGRATED TOUCH-AND-GO VALIDATION

The autonomous, closed-loop, thruster-controlled Formation Control Testbed (FCT) [10] was used to demonstrate sampling of a representative comet surface for a TAG Concept of Operations as shown in Figure 33. The robotic spacecraft with attached BiBlade tool floated on air bearings and autonomously performed the integrated proximity operations and sampling using flight-like control algorithms. The tests used the JPL Lander Vision System (LVS) [11,12,13] with the Minimal State Augmentation Algorithm

for Vision-Based Navigation (MAVeN) algorithm[14] for terrain-relative sensing and state estimation.

Demonstrations with the sampling tool on the FCT robot showed repeatable performance of the autonomous trigger to detect surface contact without a dedicated sensor, instead using post-contact control error signal buildup compared against a threshold of position error. It was shown that the sampling force to cut and sample the simulant imparted a disturbance onto the thruster-controlled robot that was easily within the authority of the 2-lb thrusters and attitude/flight-path control algorithms. The only appreciable dynamic disturbances occurred when an intentionally hard sample was not penetrable by the tool. In this case the disturbance imparted on the 450 kg robot was still within reasonable dynamic limits for the autonomous control system to arrest the imparted Delta-V and maintain spacecraft safety. This reactive disturbance is equivalent to 6 cm/s on a full-scale CONOPS spacecraft of 2200 kg.

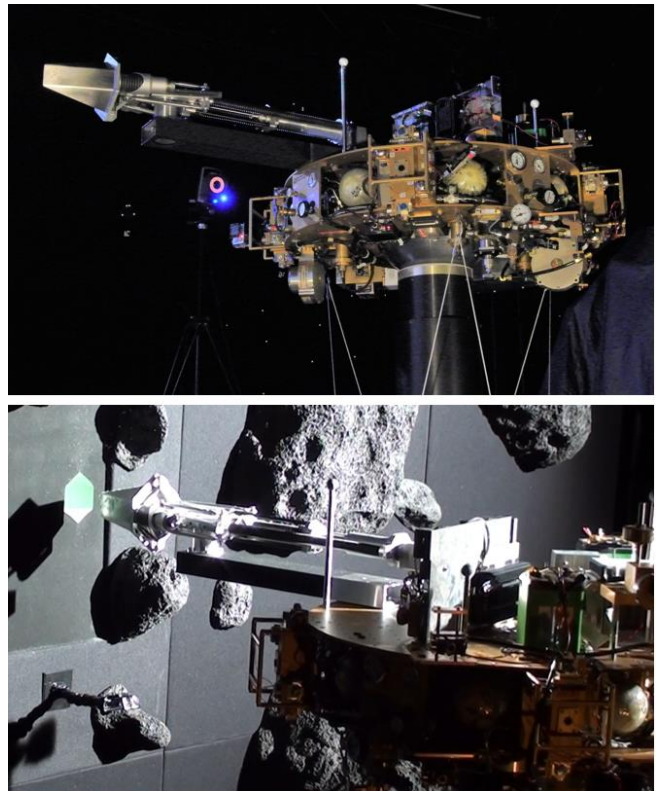


Figure 33. Integrated proximity operations and sampling in the FCT. BiBlade mounted on the air-levitated robotic spacecraft which demonstrated an autonomous Touch-and-Go approach, sampling, and ascent.

11. END-TO-END SAMPLE CHAIN VALIDATION

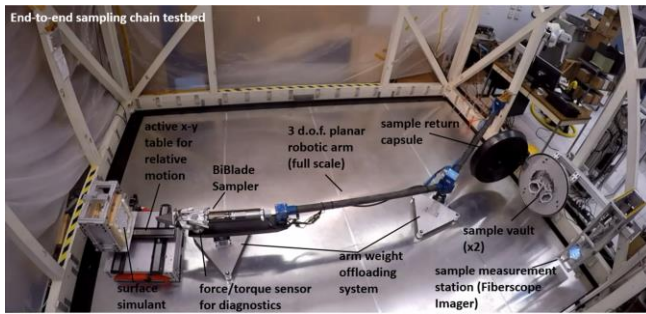


Figure 34. End-to-end sampling chain testbed.

The end-to-end sample chain was validated with the prior version of the BiBlade sampling tool and reported in [3]. The validation tests were performed in the End-to-end testbed shown in Figure 34. The end-to-end validation steps are shown in Figure 35. A full-scale robotic arm deployed the BiBlade sampling tool to a fixed position. An X-Y table moved the MPACS comet simulant to the tool and upon contact the tool fired to acquire the sample. The arm moved the tool to the sample measurement station where the sample was measured, and then the sample was deposited in a sample chamber in the Sample Return Capsule.

The end-to-end validation used the Fiberscope Sample Imaging system [3, 6] for sample measurement which would be a dedicated sample measurement station located on the spacecraft. Such a sample measurement station would be an optional element of a CSSR mission since it is expected that sample presence could be adequately determined without a dedicated sample measurement station. Sample presence in the blades could be determined from available information including the comet surface before and after sampling via imaging, blade trajectory, and spacecraft motion. The TRL 6 BiBlade uses a string potentiometer to provide measurement of blade trajectory. A flight-equivalent LVDT is expected to be used in its place.

12. FUTURE PLANS

13.1 Full-scale Testbed

A full-scale testbed is being fabricated to enable end-to-end validation of Touch-and-Go (TAG) sampling, sample measurement, and sample transfer to a Sample Return Capsule (SRC). Each of these capabilities has been sufficiently validated using the existing testbeds. This testbed will enable end-to-end validation in one testbed.

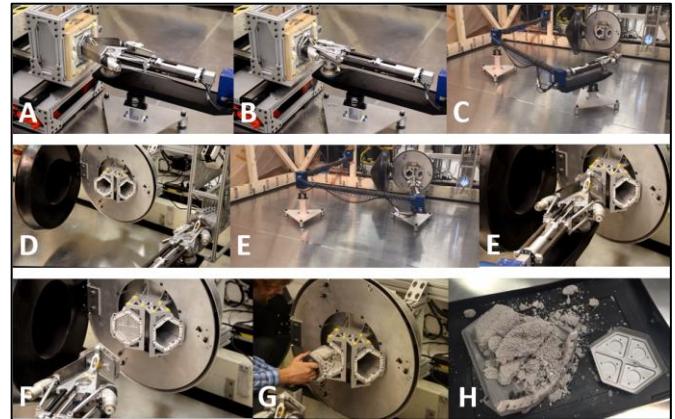


Figure 35. End-to-end sample chain test sequence. (A) Simulant block approaches. (B) Sampler blades triggered and rapidly close (~40ms) for sampling. (C) Robotic arm retracts and inserts BiBlade into Sample Measurement Station. (D) Sample measurement via fiberscope images. (E) Robotic arm inserts BiBlade into an SRC vault. (E) Blades retract leaving sample in vault and Frangibolt releases lid to seal sample. (F) BiBlade moves away from SRC. (G) Opening of sample vault to show acquired sample. (H) Full sample of MPACS simulant displayed.

Sample acquisition testing using the full-scale testbed will refine knowledge of the sampling capability of the BiBlade when attached to the spacecraft. Sampling tests using the Sample Acquisition System Testbed and Rigid Testbed provided bounding capabilities of the sampling tool. It is believed that the compliance in the Sample Acquisition System Testbed resulted in lower sampling performance, and the Rigid Testbed produced upper end sampling capabilities. Tests on the full-scale testbed will refine knowledge of the tool sampling capability, which is anticipated to be between the capabilities shown on the two other testbeds.

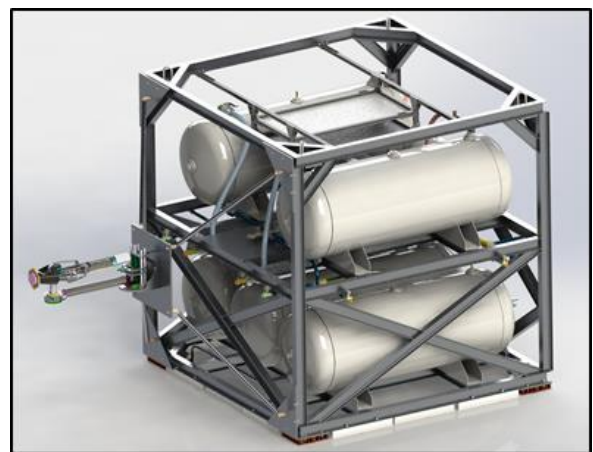


Figure 36. Full-scale air-levitated spacecraft emulator (2200 kg) is being constructed for integrated validation of Touch-and-Go dynamic sampling.

The spacecraft emulator will have representative spacecraft weight of about 2200 kg and will float on air bearings. Initially the testbed will be used for TAG sampling validation over various approach conditions and simulant strengths. For these initial tests, the tool will be mounted directly to the spacecraft structure in a way that is representative of the mounting stiffness for the mission, as shown in Figure 36. A robotic arm will be added to deploy the sampling tool and TAG sampling tests will be repeated. The SRC will be added to the spacecraft testbed and then the end-to-end sampling chain will be validated again.

13.2 Ejecta Testing

The results of the ejecta test shown in Figure 23 were affected, and potentially dominated, by air motion. Future tests to validate that minimum amount of ejecta is generated during sampling are planned to be conducted in a vacuum chamber to eliminate the effect of air motion.

13. CONCLUSIONS

The BiBlade sample chain was developed and validated to TRL 6. The tool was designed with flight design rules and cases of flight non-compliance were documented and flight implementation options were described. Validation results confirm that the tool is very robust for sampling in Comet Surface Sample Return mission scenarios. The next version of the tool could be an engineering model for a mission.

The BiBlade has many capabilities and features that make it a desirable tool for a CSSR mission, while having a relatively simple mechanical design with only one actuator and two Frangibolts. The tool enables return of two samples from different locations on a comet, including subsurface samples. Use of thin blades that are driven into the comet surface enables minimized effect on the sample. Tool geometry and blade pull-back forces ensure blade detachment from the comet for incomplete sampling cases. The tool can acquire samples over a wide range of mechanical properties and survives off-nominal operational conditions.

ACKNOWLEDGEMENTS

The research described in this publication was carried out at the Jet Propulsion Laboratory, California Institute of Technology, under a contract with the National Aeronautics and Space Administration (NASA). The work was performed as part of a task in the NASA Maturation of Instruments for Solar System Exploration program. Sampling requirements associated with science for comet surface sample return were provided by Carol Raymond and Mathieu Choukroun.

REFERENCES

- [1] Vision and Voyages for Planetary Science in the Decade 2013-2022, Committee on the Planetary Science Decadal Survey, National Research Council, The National Academies Press, 2011.
- [2] G. H. Fountain, et al., "Comet Surface Sample Mission Study", SDO-11998, prepared for NASA's Planetary Science Division, April 30, 2008.
- [3] P. Backes, et al., "Experimental Results with the BiBlade Sampling Chain for Comet Surface Sampling," IEEE Aerospace Conference, March 5-12, 2016, Big Sky, Montana.
- [4] P. Backes, et al., "Sampling System Concepts for a Touch-and-Go Architecture Comet Surface Sample Return Mission," AIAA Space, 4-7 August 2014, San Diego, California
- [5] Moreland, Diaz Lankenau, De Candido, Badescu, Backes "Penetration Mechanics Modeling & Validation of Blade Implements into Porous, Brittle Comet Simulant", IEEE Aerospace Conference, March 4-11, 2017, Big Sky, Montana.
- [6] R. Toda, et al., "FiSI: Fiberscope Sample Imaging System for Robotic Comet Surface Sample Return Missions," 2016 IEEE Aerospace Conference, March 5-12, 2016, Big Sky, Montana.
- [7] E. Carey, et al., "Comparison of Mechanical Porous Ambient Comet Simulants (MPACS) to Other Comet Surface Analog Materials," Lunar and Planetary Science Conference, abstract #2754, The Woodlands, Texas, March 20-24, 2017.
- [8] T. Spohn, et al., "Thermal and mechanical properties of the near-surface layers of comet 67P/Churyumov-Gerasimenko," *Science*, vol. 349, no. 6247, 2015.
- [9] J. Biele, et al., 2015. The landing (s) of Philae and inferences about comet surface mechanical properties. *Science*, 349(6247), p.aaa9816.
- [10] Scharf, Keim, and Hadaegh, "Flight-Like Ground Demonstrations of Precision Maneuvers for Spacecraft Formations—Part I and II", IEEE SYSTEMS JOURNAL, VOL. 4, NO. 1, MARCH 2010
- [11] Johnson et al., "Design and Ground Test Results for the Lander Vision System", AAS 13-042
- [12] Johnson, Chang, Montgomery, Trawny, Tweddle, and Zheng, "Real-Time Terrain Relative Navigation Test Results from a Relevant Environment for Mars Landing", AIAA SciTech 2015
- [13] Johnson, Aaron, Chang, Cheng, Montgomery, Mohan, Schroeder, Tweddle, Trawny, and Zheng, "The Lander Vision System for Mars 2020 Entry Descent and Landing", AAS Rocky Mountain Section Guidance, Navigation, and Control Conference, 2017.

BIOGRAPHY



Paul Backes, Ph.D. is the Group Supervisor of the Robotic Manipulation and Sampling group at Jet Propulsion Laboratory, where he has been since 1987. He received the BSME degree at U.C. Berkeley in 1982 and Ph.D. in ME from Purdue University in 1987. His awards include NASA Exceptional Engineering Achievement Medal (1993), JPL Award for Excellence (1998), NASA Software of the Year Award (2004), IEEE Robotics and Automation Award (2008), and NASA Exceptional Service Award (2014).



Scott Moreland, Ph.D. received the B.S. degree from University of Toronto and M.S. and Ph.D. degrees in Mechanical Engineering from Carnegie Mellon University and joined JPL in 2013. His expertise is primarily in robotic systems that interact with the ground for mobility or sampling. His experience includes the design and fielding of robotic vehicles, mechanism design, and mechanical systems testing.



Fredrik Rehnmark is a senior systems engineer at Honeybee Robotics. He received his Master of Science in Mechanical Engineering degree from University of California at Berkeley.



Mircea Badescu, Ph.D. is a Technologist in the NDEAA lab at JPL. He joined JPL in 2005. He received the Ph.D. degree in robotics in mechanical and aerospace engineering from Rutgers University in 2003. Prior to graduate school he worked for the Romanian Navy on the design of underwater diving equipment. He has experience with power ultrasonic piezoelectric devices, planetary and low gravity sampling systems, extreme environments devices, instruments for planetary exploration, optical components for telescopes, and optimal design of self-reconfigurable robots using parallel platforms as modules.



Kris Zacny, Ph.D. is Vice President and Director of Exploration Technology Group at Honeybee Robotics. His interests include robotic drilling, excavation, sample handling and processing, and geotechnical systems. In his previous capacity as an engineer in South African mines, Dr. Zacny managed numerous mining projects and production divisions. He received his Ph.D. at U.C. Berkeley in Mars drilling and ME in Petroleum Engineering. He participated in several Arctic and the Antarctic drilling expeditions. Dr. Zacny

has over 100 publications, including an edited book titled "Drilling in Extreme Environments: Penetration and Sampling on Earth and Other Planets".



Robert Wei is a Project Engineer at Honeybee Robotics. He received a Bachelor's degree and a Master of Engineering degree in Mechanical Engineering from Cornell University. His graduate work focused on controls and dynamics in robotic systems.



Grayson Adams joined Honeybee Robotics in the fall of 2015 where he works as a Mechanical Engineer on unique sampling and drilling systems. He received his B.S degree in mechanical engineering from the University of Southern California, where he is also currently pursuing an M.S. in Mechanical Engineering.



Risaku Toda, Ph.D. received a B.S. degree in Applied Physics and a Ph.D. degree in mechatronics and precision engineering from Tohoku University, Sendai Japan. He also received a M.S. degree in materials science and engineering from University of California Los Angeles. Prior to joining Jet Propulsion Laboratory, he worked for Ford Motor Company Japan Ltd. and a semiconductor/MEMS startup company in Texas. Since 2003, he has been with Nano and Micro Systems group at JPL. His research interests include fabrication of MEMS sensors, actuators and nanotechnology devices for aerospace applications. He holds several US patents.



Peter Vieira joined the Robotic Manipulation and Sampling group at JPL in August 2014. He received his Master of Science in Electrical & Computer Engineering at Georgia Institute of Technology where he held a Graduate Research Assistantship, during which he was a main team member of their DARPA Robotics Challenge team, Hubo. He develops controls and autonomy for planetary manipulation and sampling.



Elizabeth Carey is a member of the Planetary Ices group at Jet Propulsion Laboratory. She joined JPL in 2013 after receiving a B.S. degree in Astrophysics and a Master of Science degree in Physics from California State University, Northridge. Her graduate work focused on the morphology of vapor deposited ice into regolith under Martian conditions. Currently, she is the Research Lead of the Geo Analogs task for Mars 2020 and is also involved with multiple laboratory experiments studying the thermal and mechanical properties of ices.



Robert Krylo, P.E., is a mechanical engineer with 38 years of thermal control experience in the aerospace industry. At JPL has worked on a variety of systems including a methane heat pipe for an interferometer, a single-phase Freon loop for a Mars lander, a suspended, low mass heater for highly stable mirror control, thermal control systems for Earth-orbiting radiometers, and a passive thermal control system for a Mars spectrometer. Earlier work at Aerojet ElectroSystems included thermoelectric cooling for a focal plane and design of temperature-controlled microwave calibration targets. Robert has a M.S. in Engineering degree from California Polytechnic University, Pomona.



Miguel San Martin received his B.S. degree in Electrical Engineering from Syracuse University in 1982, and his M.S. degree in Aeronautics and Astronautics Engineering from the Massachusetts Institute of Technology in 1985. He joined JPL in 1985.



Erik S. Bailey has S.B. and S.M. degrees in Aeronautics and Astronautics from MIT and 16 years of Entry, Descent, and Landing experience at JPL where he is currently the Technical Supervisor of the Entry, Descent, and Landing (EDL) Guidance, Navigation, and Control (GNC) Systems group. He contributed to the MER, MSL, and Mars Phoenix flight projects as well as the Low Density Supersonic Decelerator (LDSD) and Autonomous Landing and Hazard Avoidance Technology (ALHAT) programs.



Carl Seubert, Ph.D. is a technical member of the Guidance and Control Analysis group at JPL. He manages the Spacecraft Formation Control Testbed. Using high fidelity simulations and hardware in the loop testing he designs autonomous guidance and control algorithms for a variety of space applications. He joined JPL in 2012.



Dylan Conway is a PhD student in Aerospace Engineering at Texas A&M University's Land, Air, and Space Robotics Lab. His research focus is on estimation, computational vision, and navigation. He is a NASA Space Technology Research Fellow and has a BSME from University at Buffalo.



Seth Aaron is a Guidance and Control Engineer at JPL with a Masters degree in Electrical and Computer Engineering from Carnegie Mellon University. At CMU he focused on control system analysis and estimation theory. Currently he is working at JPL in simulation development and analysis on the Mars 2020 DSEDS EDL Simulation and on the Mars 2020 Lander Vision System.



Harish Manohara, Ph.D. is the Deputy Manager of Instrument Electronics and Sensors section at JPL. He received a B.E. in instrumentation Technology from the Bangalore University, India in 1989, followed by an M.S. in Nuclear Engineering in 1992, and a Ph.D. in Engineering Science in 1997 from the Louisiana State University. His awards include the Lew Allen Award for Technical Excellence (2007), the Explorer Award (2015), and the NASA Exceptional Technology Achievement Medal (2016).



Gregory H. Peters is a member of the Geophysics and Planetary Geosciences Section at the Jet Propulsion Laboratory. Currently he is a Surface Sampling and Science (SSS) Scientist for the Mars Science Laboratory mission and the Cognizant Engineer of the Geo-Analogs task for the Mars2020 Mission. He joined JPL in 2001.



Marco Mongelli received the Bachelor of Engineering degree in Mechanical Engineering from the Politecnico di Torino, Italy, followed by a M.S. degree both Mechanical and Mechatronic Engineering Master's Degrees as a result of the partnership between the Polytechnic of Turin and the University of Illinois at Chicago.



Dario Riccobono received the B.S. degree from Politecnico di Torino (Italy), where he is currently pursuing an M.S. in Aerospace and Astronautic Engineering. He is working at JPL on the control system for a full-scale spacecraft emulator for a potential comet sample return mission.